



Article

# Combined Effects of Elevated Temperature and Crude Oil Pollution on Oxidative Stress and Apoptosis in Sea Cucumber (*Apostichopus japonicus*, Selenka)

Xishan Li <sup>1,2,3</sup> , Chengyan Wang <sup>2</sup>, Nan Li <sup>1,2</sup>, Yali Gao <sup>4</sup>, Zhonglei Ju <sup>1,2</sup>, Guoxiang Liao <sup>1,3,\*</sup> and Deqi Xiong <sup>2</sup>

<sup>1</sup> National Marine Environmental Monitoring Center, Dalian 116023, China; lxsdmu@outlook.com (X.L.); ln15542525989@163.com (N.L.); jzl621925@163.com (Z.J.)

<sup>2</sup> College of Environmental Science and Engineering, Dalian Maritime University, Dalian 116026, China; monicachengyan@126.com (C.W.); xiongdq@dmlu.edu.cn (D.X.)

<sup>3</sup> State Environmental Protection Key Laboratory of Coastal Ecosystem, Dalian 116023, China

<sup>4</sup> School of Marine Engineering, Jimei University, Xiamen 361021, China; yali\_gao77@outlook.com

\* Correspondence: gxiao@nmemc.org.cn; Tel.: +86-0411-8478-3810

**Abstract:** Currently, global climate change and oil pollution are two main environmental concerns for sea cucumber (*Apostichopus japonicus*) aquaculture. However, no study has been conducted on the combined effects of elevated temperature and oil pollution on sea cucumber. Therefore, in the present study, we treated sea cucumber with elevated temperature (26 °C) alone, water-accommodated fractions (WAF) of Oman crude oil at an optimal temperature of 16 °C, and Oman crude oil WAF at an elevated temperature of 26 °C for 24 h. Results showed that reactive oxygen species (ROS) level and total antioxidant capacity in WAF at 26 °C treatment were higher than that in WAF at 16 °C treatment, as evidenced by 6.03- and 1.31-fold-higher values, respectively. Oxidative damage assessments manifested that WAF at 26 °C treatment caused much severer oxidative damage of the biomacromolecules (including DNA, proteins, and lipids) than 26 °C or WAF at 16 °C treatments did. Moreover, compared to 26 °C or WAF at 16 °C treatments, WAF at 26 °C treatment induced a significant increase in cellular apoptosis by detecting the caspase-3 activity. Our results revealed that co-exposure to elevated temperature and crude oil could simulate higher ROS levels and subsequently cause much severer oxidative damage and cellular apoptosis than crude oil alone on sea cucumber.

**Keywords:** crude oil; elevated temperature; sea cucumber; oxidative stress; apoptosis



**Citation:** Li, X.; Wang, C.; Li, N.; Gao, Y.; Ju, Z.; Liao, G.; Xiong, D. Combined Effects of Elevated Temperature and Crude Oil Pollution on Oxidative Stress and Apoptosis in Sea Cucumber (*Apostichopus japonicus*, Selenka). *Int. J. Environ. Res. Public Health* **2021**, *18*, 801. <https://doi.org/10.3390/ijerph18020801>

Received: 7 December 2020

Accepted: 14 January 2021

Published: 19 January 2021

**Publisher's Note:** MDPI stays neutral with regard to jurisdictional claims in published maps and institutional affiliations.



**Copyright:** © 2021 by the authors. Licensee MDPI, Basel, Switzerland. This article is an open access article distributed under the terms and conditions of the Creative Commons Attribution (CC BY) license (<https://creativecommons.org/licenses/by/4.0/>).

## 1. Introduction

Sea cucumber (*Apostichopus japonicus*, Selenka) is one of the typical marine benthic species, mainly inhabiting along the Northern Pacific coast (e.g., Russia, Japan, and northern China) [1,2]. For its high value in nutrition and pharmaceuticals, sea cucumber is considered as one of the most commercially valuable species among seafoods [3]. It has become one of the most numerous aquaculture species in China, with a total annual production of over 210,000 t in 2018 [4,5]. Generally, sea cucumber is mainly cultured by pond farming, pen culture, and sea ranching in the coastal zones of the Bohai Sea and the Yellow Sea of China [2,6]. However, these areas are often easily threatened by human activities (e.g., urban runoff, operational discharges, and offshore drilling) and seasonal environmental stresses (e.g., elevated temperature and low salinity) [2,6,7], leading to a huge economic loss in the aquaculture industry of sea cucumber. Moreover, sea cucumber is also an important marine benthic nutrient recycler and plays an essential role in marine ecosystem [8,9]. Once the growth and survival of sea cucumber or even their recruitment are grossly affected, it may directly impact the energy cycle of marine ecosystem and cause severe resource degradation in marine environment [10]. Furthermore, numerous studies have also suggested that sea cucumber, with high acute sensitivities to environmental

changes, is a suitable candidate model organism for studying the effects of environmental stresses on marine benthos [5,11–13].

More recently, with the ever-increasing global production and consumption of crude oil, oil pollution derived from harbors, shipping, and offshore drilling could severely threaten marine ecological system and marine economy [14–16]. For instance, in July 2010, approximately 1500 t of crude oil was spilled from the Xingang Port of Dalian (China) into the Yellow Sea, leading to significant economic losses in the marine aquaculture industry in Liaoning Province, especially in sea cucumber culture [2]. From June to July 2011, a series of oil spill accidents (named the 2011 Bohai Bay Oil Spill) polluted over 840 km<sup>2</sup> of sea area and caused direct economic losses up to CNY 12.56 billion in northern China [17]. Due to its limited or null motility, sea cucumber is generally under a greater threat from oil pollution than the migratory species with the ability to escape, such as fishes [2]. Besides, for recent several decades, global climate change has caused observable ocean warming due to carbon emissions from human activities [18]. With the high dependence of marine aquaculture on water temperature, ocean warming could severely threaten marine aquaculture ecosystem and production worldwide [19,20]. As the *Apostichopus japonicus* is a temperate species (optimal water temperature: 14–18 °C) and mainly cultured in shallow water, the influence of seasonal temperature fluctuations on sea cucumber could be much more obvious than other marine aquaculture species [21,22]. Hence, elevated water temperature (over 25 °C) in summer is one of the most major challenges for sea cucumber aquaculture. For instance, in July and August 2018, extremely high temperature (exceeding 32 °C) caused higher than 90% mortality of sea cucumber in many aquaculture ponds of northern China, especially for Shandong and Liaoning Peninsula, resulting in enormous economic losses [23,24]. Previous studies have reported that elevated temperature may alter the environmental distribution of oil and its biological effects on marine organisms, consequently intensifying the adverse impact on their survival or even population recruitment [25,26]. Taken together, elevated temperature and oil pollution have been considered as two main environmental concerns for sea cucumber culture. Much attention is necessary to explore the combined effects of elevated temperature and oil pollution on the physiological responses of sea cucumber.

Although crude oil comprises thousands of organic compounds, polycyclic aromatic hydrocarbons (PAHs) are generally known as the predominant toxic components of crude oil to marine organisms [27,28]. Several recent studies have reported that oil-derived PAHs could stimulate reactive oxygen species (ROS) production during their biotransformation, resulting in an elevation of ROS levels in marine organisms [2,29,30]. Overelevation of ROS levels could further induce oxidative damage of the biomacromolecules (including DNA, proteins, and lipids) [31,32], which is known as the primary mechanism involved in cell damage, apoptosis, and tissue injury in marine organisms exposed to oil-derived PAHs [29,33–36]. Additionally, numerous studies have documented that elevated temperature could cause physiological (e.g., increased oxygen consumption) and histological (e.g., tissue injury) changes in marine organisms, and it has been suggested that elevated temperature could also disturb the balance between endogenous and exogenous ROS levels and thereby cause an incapacity of the antioxidant defense system [23,37–41]. However, until now, only a limited number of novel studies have investigated the combined effects of elevated temperature and crude oil exposure on marine organisms, such as mahi-mahi (*Coryphaena hippurus*), polar cod (*Boreogadus saida*), and Atlantic cod (*Gadus morhua*) [26,42–45]. For example, mahi-mahi in early-life stages exposed to *Deepwater Horizon* (DWH) crude oil and elevated temperature (30 °C) showed significant differences in physiological responses, such as oxygen consumption, cardiac function, and overall survival, compared to exposure to DWH crude oil alone [26,42]. To the best of our knowledge, there is no available information on the combined effects of elevated temperature and crude oil pollution on sea cucumber to date. Therefore, in the present study, we exposed sea cucumber to elevated temperature (26 °C) alone, Oman crude oil WAF at an optimal temperature of 16 °C, and Oman crude oil WAF at an elevated temperature of 26 °C for 24 h. The ROS level, the capacity of antioxidant defense system, oxidative

damage of the biomacromolecules, and cellular apoptosis were assessed to explore the effects of elevated temperature on the toxicity of crude oil to sea cucumber.

## 2. Materials and Methods

### 2.1. Experimental Design

Sea cucumbers *Apostichopus japonicus* (wet weight:  $26.92 \pm 13.95$  g) were obtained from Dalian Pikou sea cucumber aquaculture zoning, Liaoning Province, China ( $39^{\circ}27'$  N,  $122^{\circ}25'$  E), in June 2020. During an acclimatization period of 7 d, sea cucumbers were maintained in recirculating tanks containing around 60 L of pre-filtered natural seawater with a density of 15 per tank. The maintenance parameters were set as: Temperature  $16.0 \pm 0.5$  °C, pH  $7.9 \pm 0.2$ , salinity  $32.0 \pm 1.0$  psu, dissolved oxygen  $7.1 \pm 0.3$  mg·L<sup>-1</sup>, and a photoperiod of 14 h light/10 h dark. Sea cucumbers were fed once with the formulated feeds each day during the acclimatization period.

After the acclimatization, sea cucumbers were randomly allocated to 4 treatment groups: 3 exposure groups (elevated temperature: 26 °C; Oman crude oil WAF at an optimal temperature of 16 °C: WAF + 16 °C; and Oman crude oil WAF at an elevated temperature of 26 °C: WAF + 26 °C) and 1 Control group (pre-filtered natural seawater only at an optimal temperature of 16 °C), as described in Figure 1 (15 sea cucumbers per group). Each group was replicated 3 times. WAF solutions of Oman crude oil (a light crude oil) were prepared on the basis of the methodology proposed by the Chemical Response to Oil Spills: Ecological Effects Research Forum (CROSERF) [46] with minor modifications [47]. Briefly, WAF solutions were prepared with Oman crude oil and pre-filtered natural seawater at an oil loading rate of 5 g·L<sup>-1</sup> in 10 L glass aspirator bottles. The oil-seawater mixtures were mixed for 18 h and then settled for 6 h in the darkness. The WAF solutions were collected from the bottom of the aspirator bottles. The preparations of WAF solutions were performed in temperature-controlled rooms at  $16.0 \pm 0.5$  °C and  $26.0 \pm 0.5$  °C for WAF + 16 °C group and WAF + 26 °C group, respectively. All the solutions were freshly prepared prior to the exposure experiments. After an exposure period of 24 h, the body wall of each individual was dissected on an ice-cold Petri dish and washed with pre-cold 100 mM potassium phosphate (PBS) buffer (pH 7.4). Then, the tissue samples were frozen rapidly in liquid nitrogen and stored at  $-20$  °C and then immediately used for the subsequent biochemical analysis. The animal experiments were reviewed by the Standardization Administration of China (SAC) GB/T 35823-2018 Laboratory animals-General requirements for animal experiment [48].

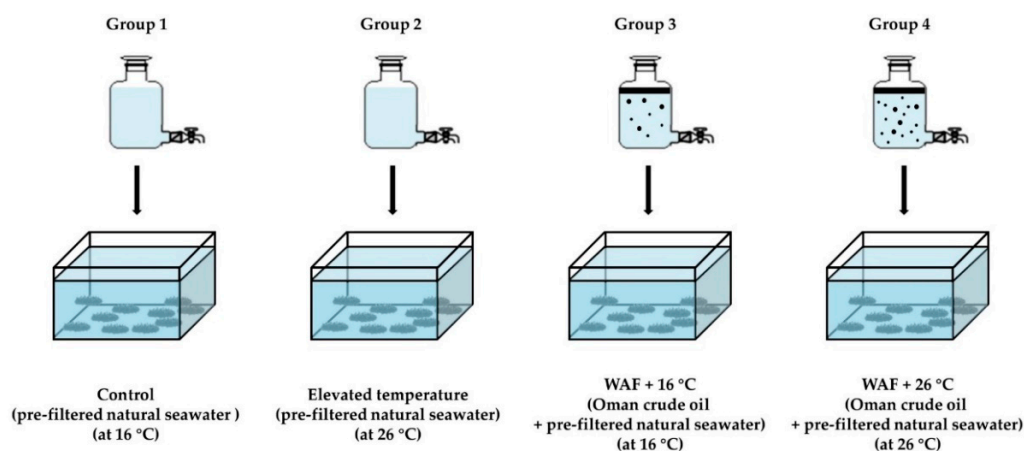


**Figure 1.** Experimental design of sea cucumber following exposure to elevated temperature (26 °C, Group 2), water-accommodated fractions (WAF) of Oman crude oil at an optimal temperature of 16 °C (WAF + 16 °C, Group 3), and Oman crude oil WAF at an elevated temperature of 26 °C (WAF + 26 °C, Group 4) for 24 h. The Control (Group 1) was the sea cucumber exposed to pre-filtered natural seawater only at an optimal temperature of 16 °C ( $n = 15$ ).

## 2.2. Analysis of Total Petroleum Hydrocarbons (TPH) and Polycyclic Aromatic Hydrocarbons (PAHs)

WAF solutions were stored at  $-20\text{ }^{\circ}\text{C}$  in the darkness until chemical analysis. Total petroleum hydrocarbons (TPH) contents of WAF solutions were determined at 225 nm with the microplate ultraviolet-visible (UV-Vis) spectrophotometer according to the SAC GB 17378.4-2007 method [49] with minor modifications as described in our previous study [50]. In brief, 200 mL of WAF solution was extracted with 2 mL of  $\text{H}_2\text{SO}_4$  solution (1:3, *v/v*) and 20 mL of *n*-hexane. The absorbance value of the extract solution at 225 nm was detected in a quartz cuvette by a microplate UV-Vis spectrophotometer (BioTek, Winooski, VT, USA). TPH concentrations of WAF solutions were calculated based on a standard curve of Oman crude oil ( $r^2 = 0.991$ ).

Additionally, the levels of United States Environmental Protection Agency (US EPA)'s 16 priority PAHs, including naphthalene (Nap), acenaphthylene (Acy), acenaphthene (Ace), fluorene (Fle), phenanthrene (Phe), anthracene (Ant), fluoranthene (Fla), pyrene (Pyr), benzo[*a*]anthracene (B[*a*]A), chrysene (Chr), benzo[*b*]fluoranthene (B[*b*]F), benzo[*k*]fluoranthene (B[*k*]F), benzo[*a*]pyrene (B[*a*]P), indeno [1,2,3-*cd*]pyrene (I[123-*cd*]P), dibenzo[*a,h*]anthracene (D[*ah*]A), and benzo[*g,h,i*]perylene (B[*ghi*]P) [51], were also analyzed according to the procedures as described in our previous works [47,52]. The pre-process of water sample (spiked with appropriate surrogate: 4-Terphenyl-d14) was performed based on the EPA 3510C liquid-liquid extraction method [53]. Then, the cleanup of the extract mixture was performed based on the EPA silica gel cleanup method [54]. Briefly, the extract mixture was dried with 4 g of granular anhydrous  $\text{Na}_2\text{SO}_4$  and concentrated to 1 mL. After that, the concentrate was transferred into a silica gel column (containing 7 g of pre-activated silica gel and 1 g of  $\text{Na}_2\text{SO}_4$ ). The collect from the silica gel column was concentrated, spiked with an internal standard mix (acenaphthene-d10, chrysene-d12, 1,4-dichlorobenzene-d4, naphthalene-d8, perylene-d12, phenanthrene-d10), and adjusted to 1 mL. Then, PAHs analysis was conducted by an Agilent 7890B gas chromatography (GC) coupled 5977A mass selective detector (MSD) (Agilent, Santa Clara, CA, USA) according to the ISO 28540:2011 method [55] with some modifications [47].

## 2.3. Reactive Oxygen Species (ROS) Level

ROS levels were detected according to the 2',7'-dichlorodihydrofluorescein diacetate (DCFH-DA) method [56]. In brief, fresh body wall tissues were homogenized in pre-cold 100 mM PBS buffer at a ratio of 1:9 (*m/v*) using a D-130 handheld homogenizer (Wiggins, Straubenhardt, Germany). The tissue homogenates were centrifuged at  $500\times g$  for 20 min at  $4\text{ }^{\circ}\text{C}$  to collect the precipitate. Then, the precipitate was incubated for 60 min at  $37\text{ }^{\circ}\text{C}$  in 1.5 mL tubes, which contained 630  $\mu\text{L}$  of PBS and 70  $\mu\text{L}$  of DCFH-DA (1 mM). The fluorescence intensities of the samples were detected under 485 nm excitation and 525 nm emission by a SpectraMax M5 multimode microplate reader (Molecular Devices, San Jose, CA, USA). The ROS levels of each sample were normalized to the total protein (TP) content and expressed in arbitrary units per mg protein ( $\text{AU}\cdot\text{mgprot}^{-1}$ ). The TP content of samples was determined at 562 nm via the microplate UV-Vis spectrophotometer based on the Bradford method [57].

## 2.4. Antioxidant Defense Capacity Assessment

To assess the capacity of antioxidant defense system, total antioxidant capacity (T-AOC) was measured in the present study based on the ferric reducing ability of plasma (FRAP) method [58]. Briefly, the body wall homogenates were centrifuged at 3000 rpm for 15 min at  $4\text{ }^{\circ}\text{C}$  to collect the supernate. Next, 4.1 mL of reaction volume (containing 200  $\mu\text{L}$  of supernate) was mixed fully and then incubated for 10 min at  $24\text{ }^{\circ}\text{C}$ . The optical density (OD) of each sample was detected at 520 nm in a quartz cuvette with the microplate UV-Vis spectrophotometer. The T-AOC was normalized to the TP content of each sample and expressed in units per mg protein ( $\text{U}\cdot\text{mgprot}^{-1}$ ).

### 2.5. Oxidative Damage Assessment

The level of oxidative DNA damage was determined using the 8-hydroxy-2'-deoxyguanosine (8-OHdG) enzyme-linked immunosorbent assay (ELISA) method [59]. In brief, 50  $\mu$ L of the body wall homogenate and 50  $\mu$ L of biotinylated antibody working solution were added into a microtiter ELISA plate well (Nanjing Jiancheng Bioengineering Institute, Nanjing, China), which had been pre-coated with an antibody specific for 8-OHdG. The ELISA plate was incubated for 30 min at 37 °C. After the incubation, each well of the ELISA plate was washed 5 times with 300  $\mu$ L PBS-Tween 20 (PBST) wash buffer. Then, 50  $\mu$ L of avidin conjugated Horseradish Peroxidase (HRP) was added into each well of the ELISA plate. The ELISA plate was incubated again for 30 min at 37 °C and then washed 5 times with 300  $\mu$ L PBST wash buffer. After washing, chromogenic solutions were added into each well and incubated for 10 min at 37 °C. Then, 50  $\mu$ L of 2 M H<sub>2</sub>SO<sub>4</sub> was added into each well to terminate the enzymatic color reaction. The OD value of each well was detected at 450 nm with the microplate UV-Vis spectrophotometer. The 8-OHdG level of each sample was calculated on the basis of a standard curve ( $r^2 = 0.972$ ), normalized to TP content, and expressed as ng per mg protein (ng·mgprot<sup>-1</sup>).

The level of protein oxidation was measured using the level of protein carbonyls (PCO), which was measured by the 2,4-dinitrophenyl hydrazine (DNPH) method [60]. Briefly, 100  $\mu$ L of the body wall homogenate and 400  $\mu$ L of 10 mM DNPH (in 2 N HCl) were mixed fully for 1 min and then incubated for 30 min at 37 °C in the dark. The reaction mixture was added with 500  $\mu$ L of trichloroacetic acid (TCA), mixed fully for 1 min, and then centrifuged for 10 min at 12,000 rpm. The precipitate was washed 4 times with 1.0 mL of ethanol/ethyl acetate (1:1, *v/v*) mixture. The final precipitate was redissolved fully in 1.25 mL of 6 M guanidine hydrochloride and then incubated for 15 min at 37 °C. After incubation, the reaction mixture was centrifuged for 15 min at 12,000 rpm. The OD value of the final supernate was detected at 450 nm with the microplate UV-Vis spectrophotometer. The PCO level of each sample was normalized to TP content and expressed as nanomoles per mg protein (nmol·mgprot<sup>-1</sup>).

Moreover, the level of lipid peroxidation was also assessed in the present study based on the content of malondialdehyde (MDA) [61]. Briefly, 200  $\mu$ L of the body wall homogenate, 200  $\mu$ L of MDA Lysis buffer, 3 mL of phosphotungstic acid solution, and 200  $\mu$ L of thiobarbituric acid (TBA) were added into a 5 mL tube and mixed fully. Then, the reaction mixture was incubated for 40 min at 95 °C, cooled in an ice bath, and centrifuged for 10 min at 4000 rpm to collect the supernate. The OD value of the supernate was detected measured at 532 nm with the microplate UV-Vis spectrophotometer. The MDA content of each sample was normalized to the TP content and expressed as nanomoles per mg protein (nmol·mgprot<sup>-1</sup>).

### 2.6. Apoptosis Assessment

The induction of cell apoptosis was evaluated according to the activity of caspase-3 [62]. In brief, 50  $\mu$ L of the body wall homogenate, 50  $\mu$ L of the Reaction Buffer (containing 10 mM DTT), and 5  $\mu$ L of the 4 mM Ac-DEVD-pNA substrate were added into a 200  $\mu$ L microcentrifuge tube and mixed well. Then, the mixture was incubated for 12 h at 37 °C. After incubation, the OD value of the mixture was detected at 400 nm with the microplate UV-Vis spectrophotometer. The relative change of caspase-3 activity of each treatment was expressed as the ratio of OD<sub>(sample)</sub>/OD<sub>(negative control)</sub>.

### 2.7. Integrated Biomarker Response (IBR) Index

To further compare the relative changes of biochemical markers in the different treatments (relative to the Control), the integrated biomarker response (IBR) indexes were calculated according to the methods as described by Beliaeff Benoit et al. [63] and modified by Sanchez Wilfried et al. [64] and Vieira et al. [65]. The deviations between different biochemical markers in different treatments ( $X_i$ ) were compared to those in the Control

( $X_0$ ). For each biochemical marker, the deviations ( $X_i/X_0$ ) were log-transformed to  $Y_i$  (Equation (1)). The general mean ( $\mu$ ) and standard deviation ( $s$ ) of all  $Y_i$  values were calculated. Then,  $Y_i$  values were normalized (Equation (2)), and the difference between  $Z_i$  and  $Z_0$  (the Control) was defined as the biomarker deviation index ( $A$ ). The  $A$  value of each biochemical marker was calculated, and the absolute values of  $A$  were added up to obtain the IBR indexes for each treatment.

$$Y_i = \log_{10} \frac{X_i}{X_0} \quad (1)$$

$$Z_i = \frac{Y_i - \mu}{s} \quad (2)$$

### 2.8. Statistical Analysis

All the results were presented as the mean  $\pm$  standard deviation (SD). Two-way analysis of variance (ANOVA) was performed to analyze the statistical difference among different treatments. Significant differences between different treatments were accepted when  $p < 0.05$  and the asterisks \*, \*\*, or \*\*\* in the graphics denoted  $p < 0.05$ , 0.01, or 0.001, respectively. Data analysis and graph plotting were conducted using GraphPad Prism Ver 8.4 (GraphPad Software, San Diego, CA, USA).

## 3. Results

### 3.1. Analysis of Total Petroleum Hydrocarbons (TPH) and Polycyclic Aromatic Hydrocarbons (PAHs)

Chemical analysis showed that TPH concentrations were  $4.59 \pm 0.07 \text{ mg}\cdot\text{L}^{-1}$  and  $5.06 \pm 0.02 \text{ mg}\cdot\text{L}^{-1}$  in the WAF solutions at  $16^\circ\text{C}$  and  $26^\circ\text{C}$ , respectively, manifesting that the TPH concentration in WAF solution at  $26^\circ\text{C}$  was 1.10-fold higher than that in WAF solution at  $16^\circ\text{C}$  ( $p < 0.01$ , Figure 2A). The contents of total 16 PAHs ( $\Sigma\text{PAHs}$ ) were  $2.31 \pm 0.45 \text{ }\mu\text{g}\cdot\text{L}^{-1}$  and  $2.91 \pm 0.58 \text{ }\mu\text{g}\cdot\text{L}^{-1}$ , respectively, indicating that the  $\Sigma\text{PAHs}$  content in WAF solution at  $26^\circ\text{C}$  was 1.26-fold higher than that in WAF solution at  $16^\circ\text{C}$  ( $p < 0.01$ , Figure 2B). Furthermore, we also analyzed the proportion (%) for each of the 16 PAHs as shown in Figure 2C. Results showed that the proportions (%) of 2-ringed, 3-ringed, 4-ringed, and  $\geq 5$ -ringed PAHs in the WAF solution at  $16^\circ\text{C}$  were 59.7%, 14.7%, 13.3%, and 12.3% of  $\Sigma\text{PAHs}$ , respectively. The proportions (%) of 2-ringed, 3-ringed, 4-ringed, and  $\geq 5$ -ringed PAHs in the WAF solution at  $26^\circ\text{C}$  were 57.6%, 17.0%, 14.9%, and 10.5% of  $\Sigma\text{PAHs}$ , respectively. Proportion analysis of these PAHs with different rings revealed that elevated temperature increased the proportion of higher molecular weight (HMW) ( $\geq 3$ -ringed), accompanied by a corresponding decrease in the proportion of lower molecular weight (LMW) PAHs (2-ringed).

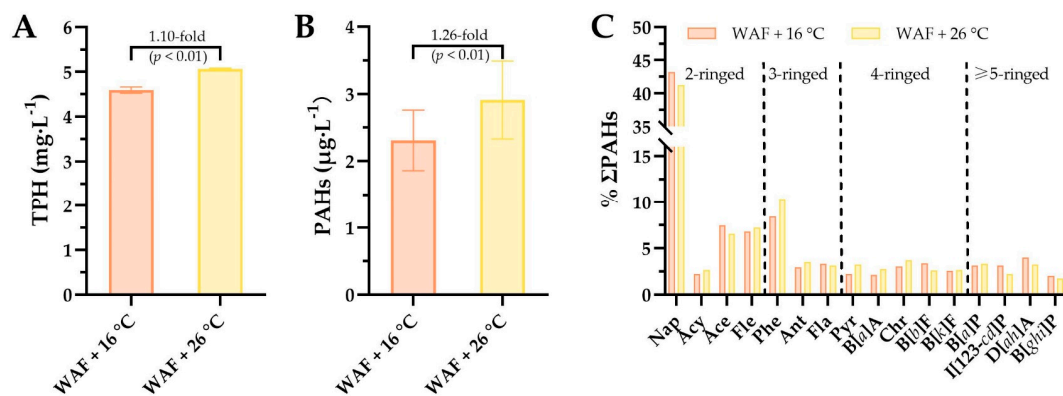


**Figure 2.** The concentrations of total petroleum hydrocarbons (TPH, (A)), the levels of US EPA's 16 priority polycyclic aromatic hydrocarbons (ΣPAHs, (B)), and the proportion (%) of each PAH (C) in the water-accommodated fractions (WAF) of Oman crude oil at an optimal temperature of 16 °C (WAF + 16 °C, light-red filled) and Oman crude oil WAF at an elevated temperature of 26 °C (WAF + 26 °C, light-yellow filled) solutions. Nap: Naphthalene, Acy: Acenaphthylene, Ace: Acenaphthene, Fle: Fluorene, Phe: Phenanthrene, Ant: Anthracene, Fla: Fluoranthene, Pyr: Pyrene, B[a]A: Benzo[a]anthracene, Chr: Chrysene, B[b]F: Benzo[b]fluoranthene, B[k]F: Benzo[k]fluoranthene, B[a]P: Benzo[a]pyrene, I[123-cd]P: Indeno[1,2,3-cd]pyrene, D[ah]A: Dibenzo[a,h]anthracene, and B[ghi]P: Benzo[g,h,i]perylene.

### 3.2. ROS Level

The ROS levels in the body wall of sea cucumber following different treatments are shown in Figure 3. The ROS levels in the 26 °C, WAF + 16 °C, WAF + 26 °C, and Control groups were  $1.07 \pm 0.11$  AU·mgprot<sup>-1</sup>,  $0.75 \pm 0.10$  AU·mgprot<sup>-1</sup>,  $4.52 \pm 0.48$  AU·mgprot<sup>-1</sup>, and  $0.21 \pm 0.03$  AU·mgprot<sup>-1</sup>, respectively, indicating that all treatments caused a significant rise in ROS levels compared to the Control (two-way ANOVA,  $p < 0.05$ ). Moreover, the ROS level in WAF + 26 °C group was 4.21- and 6.03-fold higher than that in the 26 °C group and the WAF + 16 °C group, respectively, with significant differences (two-way ANOVA,  $p < 0.001$ ).

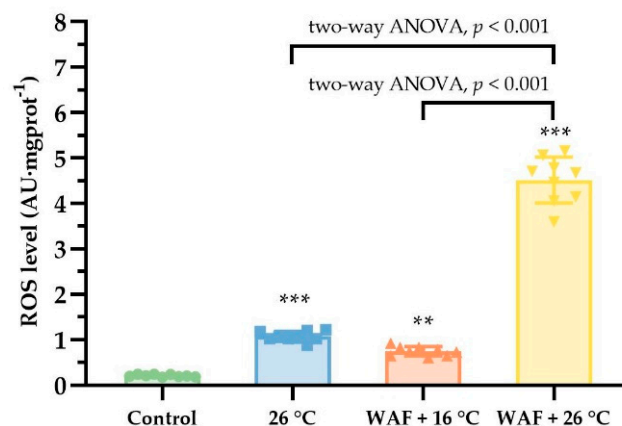


**Figure 3.** Reactive oxygen species (ROS) levels in the body wall of sea cucumber following exposure to elevated temperature (26 °C, light-blue filled square), water-accommodated fractions (WAF) of Oman crude oil at an optimal temperature of 16 °C (WAF + 16 °C, light-red filled up-triangle), and Oman crude oil WAF at an elevated temperature of 26 °C (WAF + 26 °C, light-yellow filled down-triangle). The Control was the sea cucumber exposed to pre-filtered natural seawater only at an optimal temperature of 16 °C (light-green filled circle). Error bars represent 95% confidence intervals. Asterisks (\*\*, or \*\*\*) denote the significant differences between the treatments and the Control ( $p < 0.01$ , or 0.001, respectively). Dark traits denote the significant differences among the treatments (two-way analysis of variance (ANOVA)).

### 3.3. Antioxidant Defense Capacity Assessment

The T-AOC in the body wall of sea cucumber following different treatments are shown in Figure 4. The results showed that, compared to the Control ( $0.35 \pm 0.04 \text{ U}\cdot\text{mgprot}^{-1}$ ), WAF + 16 °C treatment had no significant impact on the T-AOC ( $0.40 \pm 0.02 \text{ U}\cdot\text{mgprot}^{-1}$ ; two-way,  $p > 0.05$ ). Both 26 °C and WAF + 26 °C treatments caused a significant increase in the T-AOC ( $0.48 \pm 0.03$  and  $0.53 \pm 0.05 \text{ U}\cdot\text{mgprot}^{-1}$ , respectively) relative to the Control (two-way,  $p < 0.05$  and  $p < 0.01$ ). Additionally, WAF + 26 °C treatment had a significant higher T-AOC than 26 °C treatment but without significant differences (two-way ANOVA,  $p > 0.05$ ).

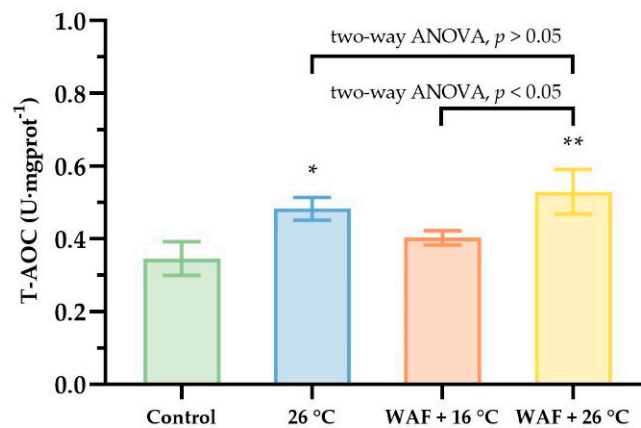


**Figure 4.** Total antioxidant capacity (T-AOC) in the body wall of sea cucumber following exposure to elevated temperature (26 °C, light-blue filled), water-accommodated fractions (WAF) of Oman crude oil at an optimal temperature of 16 °C (WAF + 16 °C, light-red filled), and Oman crude oil WAF at an elevated temperature of 26 °C (WAF + 26 °C, light-yellow filled). The Control was the sea cucumber exposed to pre-filtered natural seawater only at an optimal temperature of 16 °C (light-green filled). Asterisks (\* or \*\*) denote the significant differences between the treatments and the Control ( $p < 0.05$  or 0.01, respectively). Dark traits denote the significant differences among the treatments (two-way analysis of variance (ANOVA)).

### 3.4. Oxidative Damage Assessment

To assess the oxidative damage to macromolecules (DNA, proteins, and lipids) in body wall of sea cucumber following different treatments, the levels of 8-OHdG, PCO, and MDA were detected and are shown in Figure 5. For oxidative DNA damage (Figure 5A), results showed that the 8-OHdG levels were  $2.29 \pm 0.10 \text{ ng}\cdot\text{mgprot}^{-1}$ ,  $2.08 \pm 0.07 \text{ ng}\cdot\text{mgprot}^{-1}$ ,  $2.50 \pm 0.12 \text{ ng}\cdot\text{mgprot}^{-1}$ , and  $1.67 \pm 0.07 \text{ ng}\cdot\text{mgprot}^{-1}$  for the 26 °C, WAF + 16 °C, WAF + 26 °C, and the Control groups, respectively, indicating that all the treatments caused a significant increase in 8-OHdG level compared to the Control (two-way ANOVA,  $p < 0.001$ ,  $p < 0.01$ , and  $p < 0.001$ , respectively). The 8-OHdG level in the WAF + 26 °C group was 1.20-fold higher than that in the WAF + 16 °C group (two-way ANOVA,  $p = 0.008 < 0.01$ ), while no significant differences were observed between the 26 °C group and the WAF + 26 °C group (two-way ANOVA,  $p > 0.05$ ). As for the protein oxidation, PCO contents were detected in the present study (Figure 5B). Data showed that only WAF + 26 °C treatment caused a significant increase in the PCO content ( $6.23 \pm 0.84 \text{ nmol}\cdot\text{mgprot}^{-1}$ ) compared to the Control ( $1.55 \pm 0.31 \text{ nmol}\cdot\text{mgprot}^{-1}$ , two-way ANOVA,  $p < 0.001$ ), while the 26 °C and WAF + 16 °C treatments induced a slight rising trend but without significant differences ( $2.16 \pm 0.75 \text{ nmol}\cdot\text{mgprot}^{-1}$  and  $3.01 \pm 1.32 \text{ nmol}\cdot\text{mgprot}^{-1}$ , respectively; two-way ANOVA,  $p > 0.05$ ). Furthermore, the MDA contents were also detected as a bioindicator of lipid peroxidation in the present study (Figure 5C). Differently, compared to the Control ( $0.67 \pm 0.27 \text{ nmol}\cdot\text{mgprot}^{-1}$ ), all the treatments caused a significant elevation of MDA content, as evidenced by 1.82-, 2.07-, and



5.30-fold-higher values in the 26 °C, WAF + 16 °C, and WAF + 26 °C groups, respectively (two-way ANOVA,  $p < 0.05$ ,  $p < 0.05$ , and  $p < 0.001$ , respectively).

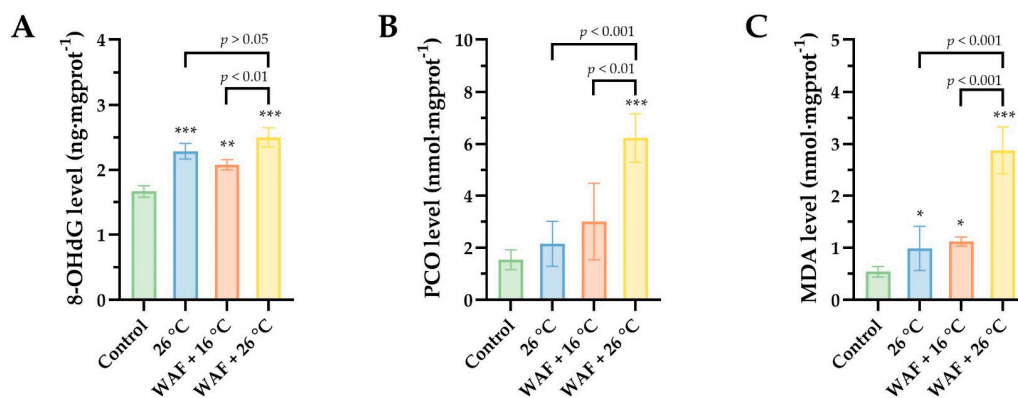


**Figure 5.** The levels of 8-hydroxy-2'-deoxyguanosine (8-OHdG) (A), protein carbonyls (PCO) (B), and malondialdehyde (MDA) (C) in the body wall of sea cucumber following exposure to elevated temperature (26 °C, light-blue filled), water-accommodated fractions (WAF) of Oman crude oil at an optimal temperature of 16 °C (WAF + 16 °C, light-red filled), and Oman crude oil WAF at an elevated temperature of 26 °C (WAF + 26 °C, light-yellow filled). The Control was the sea cucumber exposed to pre-filtered natural seawater only at an optimal temperature of 16 °C (light-green filled). Asterisks (\*, \*\*, or \*\*\*) denote the significant differences between the treatments and the Control ( $p < 0.05$ , 0.01, or 0.001, respectively). Dark traits denote the significant differences among the treatments (two-way analysis of variance (ANOVA)).

### 3.5. Apoptosis Assessment

To further evaluate the induction of cell apoptosis in the body wall of sea cucumber following different treatments, the relative changes of caspase-3 activity were measured as shown in Figure 6. The results showed that the relative caspase-3 activities in sea cucumber exposed to 26 °C, WAF + 16 °C, and WAF + 26 °C were  $2.35 \pm 0.03$ ,  $2.30 \pm 0.05$ , and  $2.53 \pm 0.06$ , which were significantly higher than that in the Control (two-way ANOVA,  $p < 0.001$ ). Moreover, the relative caspase-3 activities in the WAF + 26 °C treatment was much higher than that in the 26 °C and WAF + 16 °C treatments (two-way ANOVA,  $p < 0.001$ ).

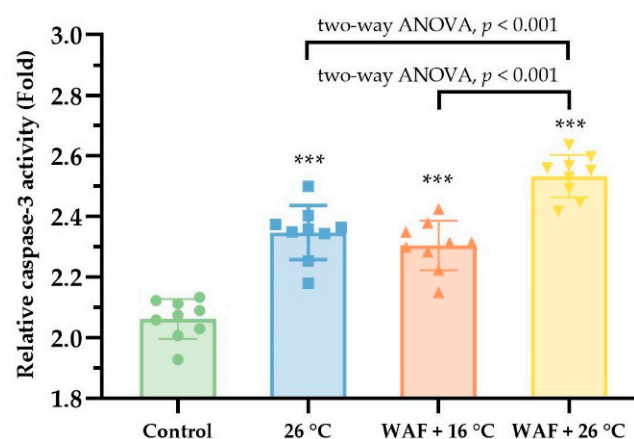


**Figure 6.** Relative caspase-3 activity (fold) in the body wall of sea cucumber following exposure to elevated temperature (26 °C, light-blue filled square), water-accommodated fractions (WAF) of Oman crude oil at an optimal temperature of 16 °C (WAF + 16 °C, light-red filled up-triangle), and Oman crude oil WAF at an elevated temperature of 26 °C (WAF + 26 °C, light-yellow filled down-triangle). The Control was the sea cucumber exposed to pre-filtered natural seawater only at an optimal temperature of 16 °C (light-green filled circle). Error bars represent 95% confidence intervals. Asterisks (\*\*\*) denote the significant differences between the treatments and the Control ( $p < 0.001$ , respectively). Dark traits denote the significant differences among the treatments (two-way analysis of variance (ANOVA)).

### 3.6. IBR Index

The results of ROS, T-AOC, 8-OHdG, PCO, MDA, and caspase-3 were further analyzed through the IBR index to assess the global responses in the body wall of sea cucumber following the 26 °C, WAF + 16 °C, and WAF + 26 °C treatments, as shown in the star plots (Figure 7). The IBR indexes were 4.58, 4.31, and 9.81 for the 26 °C, WAF + 16 °C, and WAF + 26 °C treatments, respectively, indicating that the rank of the most affected groups could be ordered as WAF + 26 °C treatment > 26 °C treatment > WAF + 16 °C treatment.

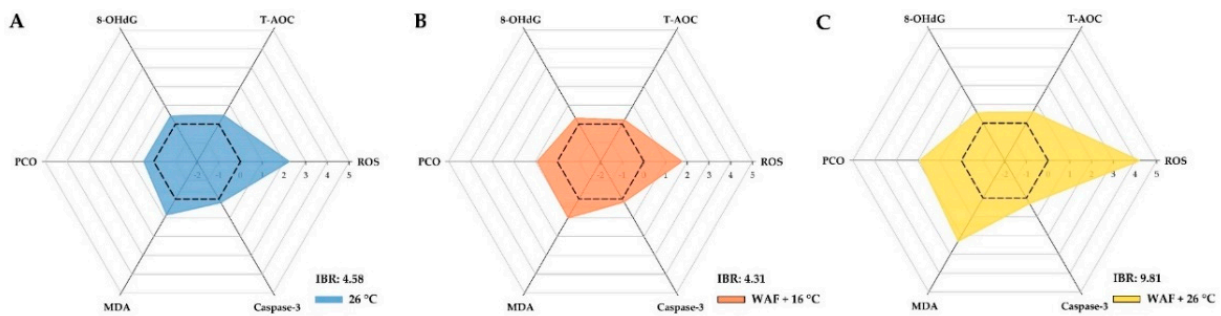


**Figure 7.** Integrated biomarker response (IBR) indexes for sea cucumber following exposure to elevated temperature (26 °C, light-blue filled, (A)), water-accommodated fractions (WAF) of Oman crude oil at an optimal temperature of 16 °C (WAF + 16 °C, light-red filled, (B)), and Oman crude oil WAF at an elevated temperature of 26 °C (WAF + 26 °C, light-yellow filled, (C)). Biomarker results are denoted relative to the Control (sea cucumber exposed to pre-filtered natural seawater only at an optimal temperature of 16 °C) (black dash lines). The area above 0 denotes the induction of the biomarker, and the area below 0 denotes the reduction of the biomarkers. ROS: Reactive oxygen species; T-AOC: Total antioxidant capacity; 8-OHdG: 8-hydroxy-2'-deoxyguanosine; PCO: Protein carbonyls; MDA: Malondialdehyde.

## 4. Discussion

In the present study, we investigated the oxidative-related changes of sea cucumber to cope with acute exposure to crude oil at an elevated temperature of 26 °C, which exceeds the optimal temperature (16 °C) for sea cucumber inhabiting. Our results showed that the cellular ROS level, as a net content of ROS in vivo regulated by the equilibrium between the ROS production and scavenging, was much higher in sea cucumber exposed to the combination of elevated temperature and crude oil (WAF at 26 °C) than that exposed to elevated temperature alone (26 °C) or crude oil alone (WAF at 16 °C), as evidenced by 4.21- and 6.03-fold higher, respectively. It indirectly suggested that elevated temperature could markedly enhance the stimulation of ROS production in sea cucumber caused by crude oil exposure, resulting in a significant induced increase in the net ROS level. Consistent with our results, previous studies have also reported that significant increases in the ROS levels of marine organisms were recorded after exposure to elevated temperature [37–39] or crude oil [2,66,67]. As a natural byproduct of oxygen metabolism, ROS, such as hydrogen peroxide (H<sub>2</sub>O<sub>2</sub>), hydroxyl radical (OH), and superoxide anion (O<sup>2-</sup>), plays an integral role in normal cell signaling and cellular function [68,69]. However, environmental stresses could increase ROS production via affecting or interrupting respiratory electron transport chains, enzymatic reaction, and other normal metabolisms [70], which could subsequently alter intracellular redox homeostasis and cause cellular oxidative stress [31,39,69,71]. To maintain the redox homeostasis within certain limits, the antioxidant enzymatic system is developed by aerobic organisms as the primary defense line for ROS scavenging, such as superoxide dismutase (SOD) and catalase (CAT) [2,69,72]. In the present study, we evaluated the antioxidant defense capacity of sea cucumber following different treatments via the T-AOC. A significant increase in the T-AOC was observed in sea cucumber following exposure to elevated temperature alone or the combination of elevated temperature and crude oil relative to the Control, as evidenced by 1.40- and 1.53-fold-higher values, respectively. In contrast, crude oil alone exposure caused a subtle increase in the T-AOC

(1.12-fold higher relative to the Control) but without a significant statistical difference. Recent studies have revealed that environmental stresses could stimulate ROS production in other marine benthos with a concomitant induced-increase in the capacity of antioxidant defense system to keep a degree of equilibrium between ROS production and scavenging [39,73,74]. Higher T-AOC observed in sea cucumber exposed to the combination of elevated temperature and crude oil than that in crude oil alone exposure might be related to the induced increase of ROS level caused by the co-exposure of the elevated temperature and crude oil. Moreover, a significant increase in the net ROS level observed in different treatments suggests that ROS production had exceeded the scavenging capacity of the antioxidant defense system in sea cucumber following different treatments, subsequently leading to the high abundance of ROS.

Excessive ROS could induce extensive oxidative damage to the biomacromolecules (e.g., DNA, proteins, and lipids), which is known as the primary mechanisms of toxic effects on marine benthos exposed to oil-derived PAHs [2,29,33]. In the present study, we detected 8-OHdG, PCO, and MDA levels in sea cucumber following different treatments to assess oxidative DNA damage, protein oxidation, and lipid peroxidation, respectively. The results showed that all the treatments resulted in various extents of increase in 8-OHdG, PCO, and MDA levels, indicating that exposure to elevated temperature, crude oil, or the combination of both could cause oxidative damage to the biomacromolecules of sea cucumber. Consistent with our study, other studies have reported that elevated temperature or crude oil exposure could induce severe oxidative damage of biomacromolecules in various marine organisms, e.g., ascidian (*Styela plicata*), polychaete (*Laeonereis culveri*), bivalve (*Anomalocardia flexuosa*), or sea cucumber (*Parastichopus regalis*) [29,75,76]. Additionally, we found that 8-OHdG, PCO, and MDA levels in sea cucumber following exposure to WAF at 26 °C were much higher than those following exposure to elevated temperature (26 °C) or WAF at 16 °C treatments, indicating that the co-exposure to elevated temperature and crude oil could cause much more severe oxidative damage to the macromolecules of sea cucumber than elevated temperature alone or crude oil alone did. Among the three biomarkers of oxidative damage, the change of MDA level in sea cucumber following different treatments was the most obvious, reinforcing the previous findings that lipid peroxidation is the relatively more sensitive biomarkers for the oxidative damage of the three main macromolecules in marine benthos under environmental stresses, especially oil-derived hydrocarbons exposure [29,33,77]. Furthermore, in the present study, we also found that relative to the Control, exposure to elevated temperature, crude oil, or the combination of both caused a significant increase in cellular apoptosis via caspase-3 activity, which is well established as one of the key executioners or final effectors for apoptosis to occur [78,79]. Cellular apoptosis is a physiological process by which the cell undergoes programmed death to eliminate redundant, unwanted, or damaged cells [74,79,80]. It is generally known that cellular apoptosis naturally occurs during cell development and aging and is a crucial survival mechanism for marine organisms under environmental stresses [29,73]. Our results supported previous findings that severe cellular apoptosis is another obvious secondary response to the overproduction of ROS in marine benthos induced by environmental stresses, which has been suggested to involve the oxidative damage of biomacromolecules, especially oxidative DNA damage [81,82]. Severe cellular apoptosis might consequently result in reducing the survival of marine benthos or even threatening their population [73].

As different biochemical markers showed different sensitivity to environmental stresses, we employed the IBR index that integrated all the biochemical responses into one index to provide a quantitative expression of the combined biochemical effects of the six biomarkers in sea cucumber following different treatments. The results showed that the IBR index of sea cucumber exposed to the combination of elevated temperature and crude oil was much higher than that exposed to elevated temperature or crude oil, which was mainly attributed to the higher induction of ROS level and MDA content. Previous studies have reported that elevated temperature could increase reaction rates as well as metabolism,

which may in turn increase the sensitivity of marine organisms to oil pollution [25,26]. This increased sensitivity could be one of the main reasons for interpreting that the co-exposure to elevated temperature and crude oil caused much severer toxic effects on sea cucumber than elevated temperature or crude oil did. Moreover, our chemical analysis revealed that the levels of TPH and  $\Sigma$ PAHs in WAF solution at 26 °C were 1.10- and 1.26-fold higher than those in WAF solution at 16 °C, especially for HMW PAHs ( $\geq 3$ -ringed) that showed a much higher proportion in WAF solution at 26 °C than that in WAF solution at 16 °C. It has been accepted that HMW PAHs are relatively strong agonists of the aryl hydrocarbon receptor (AhR) [83]. Recently, novel studies have documented that PAHs metabolism and detoxification in marine benthic invertebrates similar to the mammalian or fishes are also complex processes involved with the AhR signaling pathway, which could generate a large number of active PAHs metabolic intermediates and ROS substances [84,85]. Consistent with our study, other studies on fish species have also found that elevated temperature could acutely increase the contents of dissolved hydrocarbons from crude oil into the water column to a certain extent [44,45], which subsequently could increase the bioavailability of oil-derived hydrocarbons and lead to much more toxic effects on marine organisms [45]. We inferred that the increase of dissolved hydrocarbons caused by elevated temperature could be another main reason for the much severer toxic effects observed in sea cucumber following co-exposure to elevated temperature and crude oil.

## 5. Conclusions

Overall, in the present study, we explored the combined effects of elevated temperature and crude oil exposure on oxidative stress and apoptosis in the body wall of sea cucumber. Our results revealed that elevated temperature enhanced the stimulation of ROS production and its secondary responses related to oxidative stress caused by crude oil to sea cucumber. We speculated that elevated temperature could increase PAHs metabolism in sea cucumber and the sensitivity of sea cucumber to crude oil. Besides, elevated temperature also should attribute to the higher levels of dissolved hydrocarbons from crude oil into water column, subsequently increasing the bioavailability of sea cucumber to crude oil. Therefore, our results suggested that comprehensive consideration of the environmental conditions is necessary for oil toxicity testing and its risk assessments. Future research should further clarify the underlying molecular mechanisms involved in oxidative damage and apoptosis in sea cucumber following exposure to oil-derived hydrocarbons at elevated temperatures.

**Author Contributions:** Conceptualization, G.L., D.X., and X.L.; methodology, G.L. and X.L.; software, X.L.; validation, X.L., C.W. and Z.J.; formal analysis, X.L. and Y.G.; investigation, X.L., C.W., N.L., Y.G. and Z.J.; resources, G.L. and D.X.; data curation, X.L.; writing—original draft preparation, X.L.; writing—review and editing, X.L. and G.L.; visualization, X.L.; supervision, G.L. and D.X.; project administration, G.L.; funding acquisition, G.L. All authors have read and agreed to the published version of the manuscript.

**Funding:** This research was funded by the National Key Research and Development Program of China, grant number 2018YFD0900606, and the National Natural Science Foundation of China, grant numbers 42076215 and 42076167).

**Institutional Review Board Statement:** The study was conducted according to the guidelines of the Standardization Administration of China (SAC) GB/T 35823-2018 Laboratory Animals-General requirements for animal experiment.

**Informed Consent Statement:** Not applicable.

**Data Availability Statement:** Data available on request due to restrictions eg privacy or ethical.

**Acknowledgments:** The authors are grateful to the editor and the anonymous reviewers for their availability to review this work. Their valuable comments and suggestions have improved the quality of the manuscript.

**Conflicts of Interest:** The authors declare no conflict of interest.

## References

1. Hamel, J.F.; Mercier, A. Population status, fisheries and trade of sea cucumbers in temperate areas of the Northern Hemisphere. In *Sea Cucumbers: A Global Review of Fisheries and Trade*; FAO Fisheries and Aquaculture Technical Paper: Rome, Italy, 2008; pp. 257–292.
2. Li, X.; Liao, G.; Ju, Z.; Wang, C.; Li, N.; Xiong, D.; Zhang, Y. Antioxidant response and oxidative stress in the respiratory tree of sea cucumber (*Apostichopus japonicus*) following exposure to crude oil and chemical dispersant. *J. Mar. Sci. Eng.* **2020**, *8*, 547. [[CrossRef](#)]
3. Morroni, L.; Rakaj, A.; Grosso, L.; Fianchini, A.; Pellegrini, D.; Regoli, F. Sea cucumber *Holothuria polii* (Delle Chiaje, 1823) as new model for embryo bioassays in ecotoxicological studies. *Chemosphere* **2020**, *240*, 124819. [[CrossRef](#)] [[PubMed](#)]
4. Fisheries and Fisheries Administration Bureau of the Ministry of Agriculture. *China Fishery Statistical Yearbook 2018*; China Agriculture Press: Beijing, China, 2018; p. 181.
5. Huo, D.; Sun, L.; Zhang, L.; Ru, X.; Liu, S.; Yang, X.; Yang, H. Global-warming-caused changes of temperature and oxygen alter the proteomic profile of sea cucumber *Apostichopus jpn.* *J. Proteom.* **2019**, *193*, 27–43. [[CrossRef](#)] [[PubMed](#)]
6. Xia, S.; Yang, H.; Li, Y.; Liu, S.; Zhou, Y.; Zhang, L. Effects of different seaweed diets on growth, digestibility, and ammonia-nitrogen production of the sea cucumber *Apostichopus japonicus* (Selenka). *Aquaculture* **2012**, *338–341*, 304–308. [[CrossRef](#)]
7. Huo, D.; Sun, L.; Zhang, L.; Ru, X.; Liu, S.; Yang, H. Metabolome responses of the sea cucumber *Apostichopus japonicus* to multiple environmental stresses: Heat and hypoxia. *Mar. Pollut. Bull.* **2019**, *138*, 407–420. [[CrossRef](#)]
8. Purcell, S.; Conand, C.; Uthicke, S.; Byrne, M. Ecological roles of exploited sea cucumbers. *Oceanogr. Mar. Biol.* **2016**, *54*, 367–386.
9. Ding, K.; Zhang, L.; Sun, L.; Lin, C.; Feng, Q.; Zhang, S.; Yang, H.; Brinkman, R.; Lin, G.; Huang, Z. Transcriptome analysis provides insights into the molecular mechanisms responsible for evisceration behavior in the sea cucumber *Apostichopus japonicus*. *Comp. Biochem. Physiol. D-Genom. Proteom.* **2019**, *30*, 143–157. [[CrossRef](#)]
10. Pan, Y.; Zhang, L.; Lin, C.; Sun, J.; Kan, R.; Yang, H. Influence of flow velocity on motor behavior of sea cucumber *Apostichopus japonicus*. *Physiol. Behav.* **2015**, *144*, 52–59. [[CrossRef](#)]
11. Telahigue, K.; Rabeh, I.; Bejaoui, S.; Hajji, T.; Nechi, S.; Chelbi, E.; El Cafsi, M.H.; Soudani, N. Mercury disrupts redox status, up-regulates metallothionein and induces genotoxicity in respiratory tree of sea cucumber (*Holothuria forskali*). *Drug Chem. Toxicol.* **2020**, *43*, 287–297. [[CrossRef](#)]
12. Liang, L.; Chen, J.; Li, Y.; Zhang, H. Insights into high-pressure acclimation: Comparative transcriptome analysis of sea cucumber *Apostichopus japonicus* at different hydrostatic pressure exposures. *BMC Genom.* **2020**, *21*, 68. [[CrossRef](#)]
13. Xiu, M.; Pan, L.; Jin, Q. Bioaccumulation and oxidative damage in juvenile scallop *Chlamys farreri* exposed to benzo[a]pyrene, benzo[b]fluoranthene and chrysene. *Ecotoxicol. Environ. Saf.* **2014**, *107*, 103–110. [[CrossRef](#)] [[PubMed](#)]
14. Lee, K.W.; Shim, W.J.; Yim, U.H.; Kang, J.H. Acute and chronic toxicity study of the water accommodated fraction (WAF), chemically enhanced WAF (CEWAF) of crude oil and dispersant in the rock pool copepod *Tigriopus japonicus*. *Chemosphere* **2013**, *92*, 1161–1168. [[CrossRef](#)] [[PubMed](#)]
15. Tairova, Z.; Frantzen, M.; Mosbech, A.; Arukwe, A.; Gustavson, K. Effects of water accommodated fraction of physically and chemically dispersed heavy fuel oil on beach spawning capelin (*Mallotus villosus*). *Mar. Environ. Res.* **2019**, *147*, 62–71. [[CrossRef](#)] [[PubMed](#)]
16. Liu, Y.Z.; Miller, C.A.; Zhuang, Y.; Mukhopadhyay, S.S.; Saito, S.; Overton, E.B.; Morris, G.F. The impact of the Deepwater Horizon oil spill upon lung health—Mouse model-based RNA-seq analyses. *Int. J. Environ. Res. Public Health* **2020**, *17*, 5466. [[CrossRef](#)] [[PubMed](#)]
17. Pan, G.; Qiu, S.; Liu, X.; Hu, X. Estimating the economic damages from the Penglai 19-3 oil spill to the Yantai fisheries in the Bohai Sea of northeast China. *Mar. Pol.* **2015**, *62*, 18–24. [[CrossRef](#)]
18. Bindoff, N.; Cheung, W.; Kairo, J.G.; Aristegui, J.; Guinder, V.; Hallberg, R.; Hilmi, N.; Jiao, N.; Karim, M.; Levin, L.; et al. Changing ocean, marine ecosystems, and dependent communities (09 SROCC Ch05 FINAL-1). In *IPCC Special Report on the Ocean and Cryosphere in a Changing Climate*; Pörtner, H.-O., Masson-Delmotte, D.C.R., Zhai, V., Tignor, P., Poloczanska, M., Mintenbeck, E., Alegría, K., Nicolai, A., Okem, M., Petzold, J.A., et al., Eds.; Intergovernmental Panel on Climate Change (IPCC): Geneva, Switzerland, 2019; pp. 447–588.
19. Ahmed, N.; Thompson, S.; Glaser, M. Global aquaculture productivity, environmental sustainability, and climate change adaptability. *Environ. Manag.* **2019**, *63*, 159–172. [[CrossRef](#)]
20. Brander, K.M. Global fish production and climate change. *Proc. Natl. Acad. Sci. USA* **2007**, *104*, 19709–19714. [[CrossRef](#)]
21. Wang, Q.L.; Yu, S.S.; Dong, Y.W. Parental effect of long acclimatization on thermal tolerance of juvenile sea cucumber *Apostichopus japonicus*. *PLoS ONE* **2015**, *10*, e0143372. [[CrossRef](#)]
22. Yang, H.; Yuan, X.; Zhou, Y.; Mao, Y.; Zhang, T.; Liu, Y. Effects of body size and water temperature on food consumption and growth in the sea cucumber *Apostichopus japonicus* (Selenka) with special reference to aestivation. *Aquac. Res.* **2005**, *36*, 1085–1092. [[CrossRef](#)]
23. Li, C.; Fang, H.; Xu, D. Effect of seasonal high temperature on the immune response in *Apostichopus japonicus* by transcriptome analysis. *Fish Shellfish Immunol.* **2019**, *92*, 765–771. [[CrossRef](#)]
24. Huo, D.; Sun, L.; Zhang, L.; Yang, H.; Liu, S.; Sun, J.; Su, F. Time course analysis of immunity-related gene expression in the sea cucumber *Apostichopus japonicus* during exposure to thermal and hypoxic stress. *Fish Shellfish Immunol.* **2019**, *95*, 383–390. [[CrossRef](#)] [[PubMed](#)]

25. Baum, G.; Kegler, P.; Scholz-Böttcher, B.M.; Alfiansah, Y.R.; Abrar, M.; Kunzmann, A. Metabolic performance of the coral reef fish *Siganus guttatus* exposed to combinations of water borne diesel, an anionic surfactant and elevated temperature in Indonesia. *Mar. Pollut. Bull.* **2016**, *110*, 735–746. [[CrossRef](#)] [[PubMed](#)]
26. Perrichon, P.; Mager, E.M.; Pasparakis, C.; Stieglitz, J.D.; Benetti, D.D.; Grosell, M.; Burggren, W.W. Combined effects of elevated temperature and *Deepwater Horizon* oil exposure on the cardiac performance of larval mahi-mahi, *Coryphaena hippurus*. *PLoS ONE* **2018**, *13*, e0203949. [[CrossRef](#)] [[PubMed](#)]
27. Hodson, P.V. The toxicity to fish embryos of PAH in crude and refined oils. *Arch. Environ. Contam. Toxicol.* **2017**, *73*, 12–18. [[CrossRef](#)]
28. Incardona, J.P. Molecular mechanisms of crude oil developmental toxicity in fish. *Arch. Environ. Contam. Toxicol.* **2017**, *73*, 19–32. [[CrossRef](#)]
29. Barbosa, D.B.; Mello, A.d.A.; Allodi, S.; de Barros, C.M. Acute exposure to water-soluble fractions of marine diesel oil: Evaluation of apoptosis and oxidative stress in an ascidian. *Chemosphere* **2018**, *211*, 308–315. [[CrossRef](#)]
30. Wang, X.; Ren, H.; Li, X.; Chen, H.; Ju, Z.; Xiong, D. Sex-specific differences in the toxic effects of heavy fuel oil on sea urchin (*Strongylocentrotus intermedius*). *Int. J. Environ. Res. Public Health* **2021**, *18*, 499. [[CrossRef](#)]
31. Sies, H. Oxidative stress: Concept and some practical aspects. *Antioxidants* **2020**, *9*, 852. [[CrossRef](#)]
32. Lee, C.C.; Lin, Y.H.; Hou, W.C.; Li, M.H.; Chang, J.W. Exposure to ZnO/TiO<sub>2</sub> nanoparticles affects health outcomes in cosmetics salesclerks. *Int. J. Environ. Res. Public Health* **2020**, *17*, 6088. [[CrossRef](#)]
33. Hannam, M.L.; Bamber, S.D.; John Moody, A.; Galloway, T.S.; Jones, M.B. Immunotoxicity and oxidative stress in the Arctic scallop *Chlamys islandica*: Effects of acute oil exposure. *Ecotoxicol. Environ. Saf.* **2010**, *73*, 1440–1448. [[CrossRef](#)]
34. Duan, M.; Xiong, D.; Gao, Y.; Bai, X.; Xiong, Y.; Gao, X.; Ding, G. Transgenerational effects of heavy fuel oil on the sea urchin *Strongylocentrotus intermedius* considering oxidative stress biomarkers. *Mar. Environ. Res.* **2018**, *141*, 138–147. [[CrossRef](#)] [[PubMed](#)]
35. Duan, M.; Xiong, D.; Yang, M.; Xiong, Y.; Ding, G. Parental exposure to heavy fuel oil induces developmental toxicity in offspring of the sea urchin *Strongylocentrotus intermedius*. *Ecotoxicol. Environ. Saf.* **2018**, *159*, 109–119. [[CrossRef](#)] [[PubMed](#)]
36. Gao, X.; Ding, G.; Li, X.; Xiong, D. Comparison of toxicity effects of fuel oil treated by different dispersants on marine medaka (*Oryzias melastigma*) embryo. *Acta Oceanol. Sin.* **2018**, *37*, 123–132. [[CrossRef](#)]
37. Kamyab, E.; Kühnhold, H.; Novais, S.C.; Alves, L.M.F.; Indriana, L.; Kunzmann, A.; Slater, M.; Lemos, M.F.L. Effects of thermal stress on the immune and oxidative stress responses of juvenile sea cucumber *Holothuria scabra*. *J. Comp. Physiol. B* **2017**, *187*, 51–61. [[CrossRef](#)] [[PubMed](#)]
38. Parisi, C.; Guerriero, G. Antioxidative defense and fertility rate in the assessment of reprotoxicity risk posed by global warming. *Antioxidants* **2019**, *8*, 622. [[CrossRef](#)]
39. Nash, S.; Johnstone, J.; Rahman, M.S. Elevated temperature attenuates ovarian functions and induces apoptosis and oxidative stress in the American oyster, *Crassostrea virginica*: Potential mechanisms and signaling pathways. *Cell Stress Chaperon.* **2019**, *24*, 957–967. [[CrossRef](#)]
40. Perrichon, P.; Pasparakis, C.; Mager, E.M.; Stieglitz, J.D.; Benetti, D.D.; Grosell, M.; Burggren, W.W. Morphology and cardiac physiology are differentially affected by temperature in developing larvae of the marine fish mahi-mahi (*Coryphaena hippurus*). *Biology Open* **2017**, *6*, 800–809. [[CrossRef](#)]
41. Matos, B.; Martins, M.; Samamed, A.C.; Sousa, D.; Ferreira, I.; Diniz, M.S. Toxicity evaluation of quantum dots (ZnS and CdS) singly and combined in zebrafish (*Danio rerio*). *Int. J. Environ. Res. Public Health* **2020**, *17*, 232. [[CrossRef](#)]
42. Pasparakis, C.; Mager, E.M.; Stieglitz, J.D.; Benetti, D.; Grosell, M. Effects of *Deepwater Horizon* crude oil exposure, temperature and developmental stage on oxygen consumption of embryonic and larval mahi-mahi (*Coryphaena hippurus*). *Aquat. Toxicol.* **2016**, *181*, 113–123. [[CrossRef](#)]
43. Pasparakis, C.; Sweet, L.E.; Stieglitz, J.D.; Benetti, D.; Casente, C.T.; Roberts, A.P.; Grosell, M. Combined effects of oil exposure, temperature and ultraviolet radiation on buoyancy and oxygen consumption of embryonic mahi-mahi, *Coryphaena hippurus*. *Aquat. Toxicol.* **2017**, *191*, 113–121. [[CrossRef](#)]
44. Andersen, Ø.; Frantzen, M.; Rosland, M.; Timmerhaus, G.; Skugor, A.; Krasnov, A. Effects of crude oil exposure and elevated temperature on the liver transcriptome of polar cod (*Boreogadus saida*). *Aquat. Toxicol.* **2015**, *165*, 9–18. [[CrossRef](#)] [[PubMed](#)]
45. Lyons, M.C.; Wong, D.K.H.; Mulder, I.; Lee, K.; Burrige, L.E. The influence of water temperature on induced liver EROD activity in Atlantic cod (*Gadus morhua*) exposed to crude oil and oil dispersants. *Ecotoxicol. Environ. Saf.* **2011**, *74*, 904–910. [[CrossRef](#)] [[PubMed](#)]
46. Singer, M.M.; Aurand, D.; Bragin, G.E.; Clark, J.R.; Coelho, G.M.; Sowby, M.L.; Tjeerdema, R.S. Standardization of the preparation and quantitation of water-accommodated fractions of petroleum for toxicity testing. *Mar. Pollut. Bull.* **2000**, *40*, 1007–1016. [[CrossRef](#)]
47. Li, X.; Xiong, D.; Ding, G.; Fan, Y.; Ma, X.; Wang, C.; Xiong, Y.; Jiang, X. Exposure to water-accommodated fractions of two different crude oils alters morphology, cardiac function and swim bladder development in early-life stages of zebrafish. *Chemosphere* **2019**, *235*, 423–433. [[CrossRef](#)]
48. SAC. GB/T 35823-2018 Laboratory animals-General requirements for animal experiment. In *Standardization Administration of the People's Republic of China*; Standards Press of China: Beijing, China, 2018; Volume GB/T 35823-2018, p. 7.
49. SAC. GB 17378.4-2007 The specification for marine monitoring-Part 4: Seawater analysis. In *Standardization Administration of the People's Republic of China*; Standards Press of China: Beijing, China, 2007; Volume GB 17378.4-2007, pp. 44–45.

50. Li, X.; Ding, G.; Xiong, Y.; Ma, X.; Fan, Y.; Xiong, D. Toxicity of water-accommodated fractions (WAF), chemically enhanced WAF (CEWAF) of Oman crude oil and dispersant to early-life stages of zebrafish (*Danio rerio*). *Bull. Environ. Contam. Toxicol.* **2018**, *101*, 314–319. [[CrossRef](#)]
51. EPA. *Method 610: Polynuclear Aromatic Hydrocarbons*; U.S. Environmental Protection Agency (EPA): Washington, DC, USA, 1984; p. 25.
52. Li, X.; Xiong, D.; Ju, Z.; Xiong, Y.; Ding, G.; Liao, G. Phenotypic and transcriptomic consequences in zebrafish early-life stages following exposure to crude oil and chemical dispersant at sublethal concentrations. *Sci. Total Environ.* **2020**, 143053, in press. [[CrossRef](#)]
53. EPA. *Method 3510C: Separatory Funnel Liquid-Liquid Extraction*; U.S. Environmental Protection Agency (EPA): Washington, DC, USA, 1996; p. 8.
54. EPA. *Method 3630C: Silica Gel Cleanup, Part of Test Methods for Evaluating Solid Waste, Physical/Chemical Methods*; U.S. Environmental Protection Agency (EPA): Washington, DC, USA, 1996; p. 15.
55. ISO. *Water Quality-Determination of 16 Polycyclic Aromatic Hydrocarbons (PAH) in Water-Method Using Gas Chromatography with Mass Spectrometric Detection (GC-MS)*; International Organization for Standardization: Geneva, Switzerland, 2011; p. 24.
56. LeBel, C.P.; Ischiropoulos, H.; Bondy, S.C. Evaluation of the probe 2',7'-dichlorofluorescein as an indicator of reactive oxygen species formation and oxidative stress. *Chem. Res. Toxicol.* **1992**, *5*, 227–231. [[CrossRef](#)]
57. Bradford, M.M. A rapid and sensitive method for the quantitation of microgram quantities of protein utilizing the principle of protein-dye binding. *Anal. Biochem.* **1976**, *72*, 248–254. [[CrossRef](#)]
58. Benzie, I.F.F.; Strain, J.J. The ferric reducing ability of plasma (FRAP) as a measure of “antioxidant power”: The FRAP assay. *Anal. Biochem.* **1996**, *239*, 70–76. [[CrossRef](#)]
59. Valavanidis, A.; Vlachogianni, T.; Fiotakis, C. 8-hydroxy-2'-deoxyguanosine (8-OHdG): A critical biomarker of oxidative stress and carcinogenesis. *J. Environ. Sci. Health Pt. C-Environ. Carcinog. Ecotoxicol. Rev.* **2009**, *27*, 120–139. [[CrossRef](#)]
60. Levine, R.L.; Williams, J.A.; Stadtman, E.P.; Shacter, E. Carbonyl assays for determination of oxidatively modified proteins. In *Methods in Enzymology*; Academic Press: New York, NY, USA, 1994; pp. 346–357.
61. Buege, J.A.; Aust, S.D. Microsomal lipid peroxidation. In *Methods in Enzymology*; Fleischer, S., Packer, L., Eds.; Academic Press: New York, NY, USA, 1978; pp. 302–310.
62. Marissen, W.E.; Guo, Y.; Thomas, A.A.M.; Matts, R.L.; Lloyd, R.E. Identification of caspase 3-mediated cleavage and functional alteration of eukaryotic initiation factor 2 $\alpha$  in apoptosis. *J. Biol. Chem.* **2000**, *275*, 9314–9323. [[CrossRef](#)] [[PubMed](#)]
63. Beliaeff, B.; Burgeot, T. Integrated biomarker response: A useful tool for ecological risk assessment. *Environ. Toxicol. Chem.* **2002**, *21*, 1316–1322. [[CrossRef](#)] [[PubMed](#)]
64. Sanchez, W.; Burgeot, T.; Porcher, J.M. A novel “Integrated Biomarker Response” calculation based on reference deviation concept. *Environ. Sci. Pollut. Res.* **2013**, *20*, 2721–2725. [[CrossRef](#)] [[PubMed](#)]
65. Vieira, C.E.D.; Pérez, M.R.; Acayaba, R.D.A.; Raimundo, C.C.M.; dos Reis Martinez, C.B. DNA damage and oxidative stress induced by imidacloprid exposure in different tissues of the Neotropical fish *Prochilodus lineatus*. *Chemosphere* **2018**, *195*, 125–134. [[CrossRef](#)] [[PubMed](#)]
66. Olivares-Rubio, H.F.; Salazar-Coria, L.; Nájera-Martínez, M.; Godínez-Ortega, J.L.; Vega-López, A. Lipid metabolism and pro-oxidant/antioxidant balance of *Halimphora oceanica* from the Gulf of Mexico exposed to water accommodated fraction of Maya crude oil. *Ecotoxicol. Environ. Saf.* **2018**, *147*, 840–851. [[CrossRef](#)]
67. Han, J.; Kim, H.S.; Kim, I.C.; Kim, S.; Hwang, U.K.; Lee, J.S. Effects of water accommodated fractions (WAFs) of crude oil in two congeneric copepods *Tigriopus* sp. *Ecotoxicol. Environ. Saf.* **2017**, *145*, 511–517. [[CrossRef](#)]
68. Yu, B.P. Cellular defenses against damage from reactive oxygen species. *Physiol. Rev.* **1994**, *74*, 139–162. [[CrossRef](#)]
69. Rampon, C.; Volovitch, M.; Joliot, A.; Vriza, S. Hydrogen peroxide and redox regulation of developments. *Antioxidants* **2018**, *7*, 159. [[CrossRef](#)]
70. Jiang, M.; Li, L.; Li, Y.; Shen, G.; Shen, X. Oxidative stress in shellfish *Sinonovacula constricta* exposed to the water accommodated fraction of zero sulfur diesel oil and Pinghu crude oil. *Arch. Environ. Contam. Toxicol.* **2017**, *73*, 294–300. [[CrossRef](#)]
71. Di Meo, S.; Reed, T.T.; Venditti, P.; Victor, V.M. Role of ROS and RNS sources in physiological and pathological conditions. *Oxid. Med. Cell. Longev.* **2016**, *2016*, 1245049. [[CrossRef](#)]
72. Cui, Y.; Hou, Z.; Ren, Y.; Men, X.; Zheng, B.; Liu, P.; Xia, B. Effects of aerial exposure on oxidative stress, antioxidant and non-specific immune responses of juvenile sea cucumber *Apostichopus japonicus* under low temperature. *Fish Shellfish Immunol.* **2020**, *101*, 58–65. [[CrossRef](#)] [[PubMed](#)]
73. Rahman, M.S.; Rahman, M.S. Effects of elevated temperature on prooxidant-antioxidant homeostasis and redox status in the American oyster: Signaling pathways of cellular apoptosis during heat stress. *Environ. Res.* **2020**, 110428, in press. [[CrossRef](#)] [[PubMed](#)]
74. Johnstone, J.; Nash, S.; Hernandez, E.; Rahman, M.S. Effects of elevated temperature on gonadal functions, cellular apoptosis, and oxidative stress in Atlantic sea urchin *Arbacia punctulata*. *Mar. Environ. Res.* **2019**, *149*, 40–49. [[CrossRef](#)] [[PubMed](#)]
75. Braga, M.A.; Brauko, K.M.; Vicentini, M.; Salgado, L.D.; Silva de Assis, H.C.; Dolatto, R.G.; Grassi, M.T.; Sandrini-Neto, L.; Lana, P.C. Cytotoxicity and enzymatic biomarkers as early indicators of benthic responses to the soluble-fraction of diesel oil. *Ecotoxicol. Environ. Saf.* **2018**, *164*, 21–31. [[CrossRef](#)] [[PubMed](#)]
76. Galimany, E.; Baeta, M.; Ramon, M. Immune response of the sea cucumber *Parastichopus regalis* to different temperatures: Implications for aquaculture purposes. *Aquaculture* **2018**, *497*, 357–363. [[CrossRef](#)]

77. Zhou, Z.; Liu, Z.; Wang, L.; Luo, J.; Li, H. Oxidative stress, apoptosis activation and symbiosis disruption in giant clam *Tridacna crocea* under high temperature. *Fish Shellfish Immunol.* **2019**, *84*, 451–457. [[CrossRef](#)]
78. Jia, R.; Han, C.; Lei, J.-L.; Liu, B.-L.; Huang, B.; Huo, H.-H.; Yin, S.-T. Effects of nitrite exposure on haematological parameters, oxidative stress and apoptosis in juvenile turbot (*Scophthalmus maximus*). *Aquat. Toxicol.* **2015**, *169*, 1–9. [[CrossRef](#)]
79. Hengartner, M.O. The biochemistry of apoptosis. *Nature* **2000**, *407*, 770–776. [[CrossRef](#)]
80. Ahamed, M.; Akhtar, M.J.; Alhadlaq, H.A. Co-exposure to SiO<sub>2</sub> nanoparticles and arsenic induced augmentation of oxidative stress and mitochondria-dependent apoptosis in human cells. *Int. J. Environ. Res. Public Health* **2019**, *16*, 3199. [[CrossRef](#)]
81. Zhang, T.; Yan, Z.; Zheng, X.; Wang, S.; Fan, J.; Liu, Z. Effects of acute ammonia toxicity on oxidative stress, DNA damage and apoptosis in digestive gland and gill of Asian clam (*Corbicula fluminea*). *Fish Shellfish Immunol.* **2020**, *99*, 514–525. [[CrossRef](#)]
82. Alarifi, S.; Ali, D.; Y., A.O.S.; Ahamed, M.; Siddiqui, M.A.; Al-Khedhairi, A.A. Oxidative stress contributes to cobalt oxide nanoparticles-induced cytotoxicity and DNA damage in human hepatocarcinoma cells. *Int. J. Nanomed.* **2013**, *8*, 189–199.
83. Incardona, J.P.; Day, H.L.; Collier, T.K.; Scholz, N.L. Developmental toxicity of 4-ring polycyclic aromatic hydrocarbons in zebrafish is differentially dependent on AH receptor isoforms and hepatic cytochrome P4501A metabolism. *Toxicol. Appl. Pharmacol.* **2006**, *217*, 308–321. [[CrossRef](#)] [[PubMed](#)]
84. Wang, H.; Pan, L.; Zhang, X.; Ji, R.; Si, L.; Cao, Y. The molecular mechanism of AhR-ARNT-XREs signaling pathway in the detoxification response induced by polycyclic aromatic hydrocarbons (PAHs) in clam *Ruditapes philippinarum*. *Environ. Res.* **2020**, *183*, 109165. [[CrossRef](#)] [[PubMed](#)]
85. Liu, D.; Pan, L.; Li, Z.; Cai, Y.; Miao, J. Metabolites analysis, metabolic enzyme activities and bioaccumulation in the clam *Ruditapes philippinarum* exposed to benzo[*a*]pyrene. *Ecotoxicol. Environ. Saf.* **2014**, *107*, 251–259. [[CrossRef](#)]